Multioverlap Simulations of the 3D Edwards-Anderson Ising Spin Glass

Bernd A. Berg[1,2,*] and Wolfhard Janke[3,†]

[1]*Department of Physics, The Florida State University, Tallahassee, Florida 32306*
[2]*Supercomputer Computations Research Institute, Tallahassee, Florida 32306*
[3]*Institut für Physik, Johannes Gutenberg-Universität, D-55099 Mainz, Germany*

(Received 30 December 1997)

We introduce a novel method for numerical spin glass investigations: Simulations of two replica at fixed temperature, weighted to achieve a broad distribution of the Parisi overlap parameter q (multioverlap). We demonstrate the feasibility of the approach by studying the 3D Edwards-Anderson Ising ($J_{ik} = \pm 1$) spin glass in the broken phase ($\beta = 1$). This makes it possible to obtain reliable results about spin glass tunneling barriers. In addition, our results indicate a nontrivial scaling behavior of the canonical q distributions not only at the freezing point but also deep in the broken phase. [S0031-9007(98)06189-4]

PACS numbers: 75.10.Nr, 75.40.Mg, 75.50.Lk

The intuitive picture for spin glasses and other systems with conflicting constraints (for reviews see Ref. [1]) is that there exists a large number of degenerate thermodynamic states with the same macroscopic properties but with different microscopic configurations. These states are separated by free-energy barriers in phase space, caused by disorder and frustration. However, one difficulty of the theory of spin glasses is to give a precise meaning to this classification: No explicit order parameter exists which allows one to exhibit the barriers. The way out of this dilemma appears to use an implicit parametrization, the Parisi overlap parameter q, which allows one to visualize at least some of them. Calculations of the thus encountered barriers in q are of major interest. For instance, it is unclear whether the degenerate thermodynamic states are separated by infinite barriers or whether this is just an artifact of mean-field theory.

Before performing numerical calculations of these barriers, one of the questions which ought to be addressed is "What are suitable weight factors for the problem?" The weight factor of canonical Monte Carlo (MC) simulations is $\exp(-\beta E)$, where E is the energy of the configuration to be updated and β is the inverse temperature in natural units. The Metropolis and other methods generate canonical configurations through a Markov process. However, by their very definition free-energy barriers are suppressed in such an ensemble. Now, it became widely recognized in recent years that MC simulations with *a priori* unknown weight factors, like, for instance, the inverse spectral density $1/n(E)$, are also feasible and deserve to be considered; for reviews see Ref. [2]. Along such lines progress has been made by exploring [3–6] innovative weighting methods for the spin glass problem, where free-energy barriers are caused by disorder and frustration (conflicting constraints) such that canonical simulations break down below some freezing temperature.

The main idea of the studies [3–6] is to avoid getting stuck in metastable low-energy states by using a Markov process which samples the ordered as well as the disordered regions of configuration space in one run. Refreshing the system in the disordered phase clearly benefits the simulations, but the performance has remained below early expectation. One reason appears to be that the direct (i.e., ignoring the dynamics of the system) barrier weights are not affected, such that the simulation slows down due to the treelike structure of the low-energy spin glass states; see Ref. [7] for a detailed discussion. The present paper introduces a novel, efficient approach, which targets the barrier weights directly.

We focus on the 3D Edwards-Anderson Ising (EAI) spin glass on a simple cubic lattice. It is widely considered to be the simplest model to exhibit realistic spin glass behavior and has been the testing ground of Refs. [3–6]. The energy is given by

$$E = -\sum_{\langle ik \rangle} J_{ik} s_i s_k \,, \tag{1}$$

where the sum is over nearest-neighbor sites. The Ising spins s_i and s_k as well as the exchange coupling constants J_{ik} take values ± 1. A realization is defined by a fixed assignment of the exchange coupling constants J_{ik}. In our investigation we enforce the constraint $\sum_{\langle ik \rangle} J_{ik} = 0$ by picking half of the J_{ik} at random and assigning them the value $+1$, whereas the others are fixed at -1. Early MC simulations of the EAI model (for a concise review see Ref. [6]) located the freezing temperature at $\beta_c \approx 0.9$. Recent, very high statistics canonical simulations [8,9] estimate $\beta_c = 0.901 \pm 0.034$, and improve the evidence in support of a second-order phase transition at β_c.

Reference [4] combined two copies (replica) of the same realization (defined by its couplings J_{ik}) in one simulation. The purpose was to allow for direct evaluation of the Parisi overlap parameter

$$q = \frac{1}{N} \sum_{i=1}^{N} s_i^1 s_i^2 \,. \tag{2}$$

Here N denotes the number of spins, the spins $s_i^1 = \pm 1$ correspond to the first replica, and the spins $s_i^2 = \pm 1$ to the second replica. Now, our observation is that one does still control canonical expectation values at temperature β^{-1} when one simulates with a weight function

$$w = \exp\left[\beta \sum_{\langle ik \rangle} J_{ik}(s_i^1 s_k^1 + s_i^2 s_k^2) + S(q) \right]. \quad (3)$$

This is obvious for $S(q) = 0$, and a nontrivial $S(q)$ can be mapped onto this situation by reweighting [2]. Of particular interest is to determine $S(q)$ recursively [10] such that the histogram $H(q)$ becomes uniform in q and the interpretation of $S(q)$ being the microcanonical entropy of the Parisi order parameter. Hence, although an explicit order parameter does not exist, an approach very similar to the multimagnetical [11] (which is an highly efficient way to sample interface barriers for ferromagnets) exists herewith.

Our EAI simulations are performed on $N = L^3$ lattices at $\beta = 1$, in the interesting region well below the freezing temperature. All calculations were done on a cluster of Alpha workstations at FSU. We simulated 512 different realizations for $L = 4$, 6, 8, and 33 for $L = 12$. Each production run of data taking was concluded after at least twenty tunneling events of the form

$$(q = 0) \longrightarrow (q = \pm 1) \quad \text{and back}$$

were recorded. Table I gives an overview of the tunneling performance of our algorithm. Fitting the estimates of the mean value $\overline{\tau}$ to the form $\ln(\overline{\tau}) = a + z \ln(N)$ gives $z = 2.42 \pm 0.03$. As will be discussed below, the implied improvement with respect to barrier calculations is huge. Nevertheless, the slowing down is quite off from the theoretical optimum, which is $z = 1$ for multicanonical simulations [2]. One reason seems to be that we are enforcing the limit $q \to \pm 1$. It correlates strongly with ground states, which are difficult to reach by local updates; see, for instance, Ref. [7]. Being content with a smaller region (like the two outmost maxima in the q distribution) is expected to give further improvements of the tunneling performance. Other data compiled in Table I are the encountered minimum, maximum, and median tunneling times. We observe that the mean values are systematically larger than the median, which means that the tunneling distribution has a rather long tail towards large tunneling times. On the other hand, the effect is not severely hindering our multioverlap simulations: For the lattice sizes $L = 4$ to 8 the worst behaved realization took never more than 3% of the entire computer time, and for $L = 12$ (where we have only 33 realizations) this amount was 12%.

TABLE I. Overview of the tunneling performance: minimum, maximum, median, and mean ± error tunneling times. All numbers are in units of sweeps.

L	$\tau_{\min}$	$\tau_{\max}$	τ_{med}	$\overline{\tau}$
4	4.5E02	6.2E03	9.9E02	(1.13 ± 0.03)E03
6	4.9E03	3.1E05	1.3E04	(1.88 ± 0.09)E04
8	2.4E04	1.6E06	1.1E05	(1.76 ± 0.09)E05
12	7.1E05	1.6E07	2.7E06	(4.11 ± 0.65)E06

Initially in each run, a working estimate of the weight function (3) has to be obtained. Using a variant of the recursion proposed in [10] this has turned out to be remarkably easy. For each case we stopped the recursion of weights after four tunnelings were achieved and the used computer time was smaller than $4\overline{\tau}$, with $\overline{\tau}$ as given in Table I.

The analysis of the thus created data allows us to calculate a number of physically interesting quantities. In particular, accurate determinations of the canonical potential barriers in q are, for the first time, possible. Let $P_i(q)$ be the canonical probability densities of q, where $i = 1, \ldots, n$ labels the different realizations (additional dependence on lattice size and temperature is implicit). We define the corresponding potential barrier by

$$B_i = \prod_{q=-1}^{-\triangle q} \max[1, P_i(q)/P_i(q + \triangle q)], \quad (4)$$

where $\triangle q$ is the stepsize in q. For the double-peak situations of first-order phase transitions [11], Eq. (4) becomes $B_i = P_i^{\max}/P_i^{\min}$, where $P_i^{\max}$ is the absolute maximum and $P_i^{\min}$ is the absolute minimum (for ferromagnets at $q = 0$) of the probability density $P_i(q)$. Our definition generalizes to the situation where several minima and maxima occur due to disorder and frustration. When evaluating (4) from numerical data for $P_i(q)$ some care is needed to avoid contributions from statistical fluctuations of $P_i(q)$.

Graphically, our values for the B_i are presented in Fig. 1. It comes as a surprise that the finite-size dependence of the distributions is very weak. To study this issue further, we have compiled in Table II for each lattice size the following information about our potential barrier

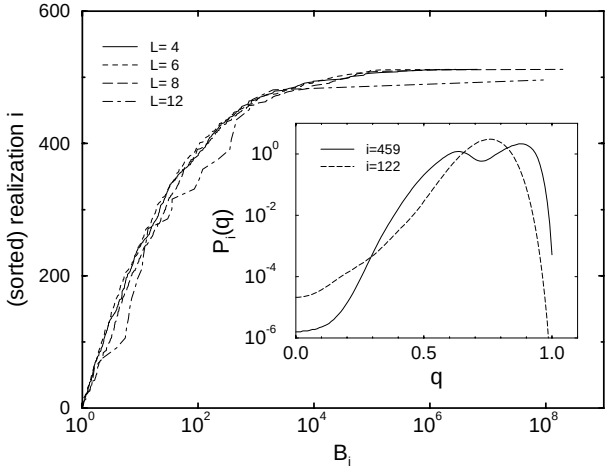

FIG. 1. Canonical tunneling barrier distributions at $\beta = 1$. (The $L = 12$ barriers are relabeled to fill into the 1–512 range.) The inset shows the two worst $L = 6$ realizations.

TABLE II. Canonical potential barriers: maximum (and its contribution to the mean in %), second largest value, upper median confidence limit, median, lower median confidence limit (upper and lower limit bound a 70% confidence interval), the mean, and its error bar.

L	$B_{\max}$	B_2	B^{+}_{med}	B_{med}	B^{-}_{med}	$\overline{B}$
4	6.56E06 (70%)	9.11E05	15.1	12.4	9.62	(1.84 ± 1.30)E04
6	2.76E06 (74%)	1.44E05	12.3	11.1	10.1	(7.29 ± 5.42)E03
8	1.97E08 (98%)	1.36E06	17.7	15.2	12.3	(3.91 ± 3.85)E05
12	9.14E07 (100%)	1.96E03	35.3	12.9	10.7	(2.77 ± 2.77)E06

results: largest and second largest values $B_{\max}$ and B_2, median values and 70% confidence limits around those, and mean values $\overline{B}$ with statistical error bars. From this table it becomes obvious why this investigation could not be performed using canonical methods to which in this context multicanonical simulations and enlarged ensembles also belong, as their weights for those barriers are still canonical. For these methods the slowing down is proportional to the average barrier height $\overline{B}$, which is already large for $L = 4$, about 18×10^3, and increases to about 2.8×10^6 for $L = 12$. On $L = 4$ and $L = 6$ systems we have performed a number of (very long) canonical simulations to estimate the proportionality constant between barrier height and improvement due to our multi-q simulations. Using these results, we estimate that with our computer program a canonical MC calculation of the worst $L = 12$ barrier alone, the one reported in Table II, would take about 1000 years on a 500 MHz Alpha processor.

The reader may be puzzled by the very large error bars assigned to the mean barrier values. Their explanation is the following: The entire mean value is dominated by the largest barrier, which contributes between 70% ($L = 4$) and, practically, 100% ($L = 12$); see $B_{\max}$ in the second column of Table II. Besides $B_{\max}$, the second largest value B_2 is listed in the third column. It may be remarked that most of these worst case barriers exhibit simple double-peak behavior. An exception is $L = 6$ where the distribution yielding $B_{\max}$ has two double peaks. To exhibit the difference, the inset of Fig. 1 depicts the right-hand side of the $L = 6$ probability densities $P_i(q)$ with $i = 459$ corresponding to the $B_{\max}$ and $i = 122$ to the B_2 barrier. For B_2 the value of our barrier definition (4) agrees with the $P_{\max}/P_{\min}$ value, whereas for $B_{\max}$ it is by about a factor of 2 larger.

Typical configurations, described by the median results of Table II, have much smaller tunneling barriers. They turn out to be quite insensitive to the lattice size; in fact, the value $B_{\mathrm{med}} = 12.3$ fits into the confidence interval for all simulated lattice sizes. Presumably, there is some increase of B_{med} with lattice size, but to trace it we would need to simulate more realizations. This result of an almost constant typical tunneling barrier is consistent with the fact that our tunneling times are rather far apart from their theoretical optimum: Still other reasons than overlap barriers have to be responsible. Therefore, one may also question the apparently accepted opinion that typical barriers are primarily responsible for the severe slowing down of canonical MC simulations.

Our data allow canonical reweighting in a β range which includes the critical temperature $\beta_c = 0.88$. By analyzing the spin glass susceptibility, $\chi_{\mathrm{SG}} = N[\langle q^2\rangle]_{\mathrm{av}}$, we obtain the best finite-size scaling fit $\chi_{\mathrm{SG}} \propto L^{\gamma/\nu}$ at $\beta = 0.88$ with $\gamma/\nu = 2.37(4)$ and a goodness-of-fit parameter $Q = 0.25$. This is corroborated by the curves of the Binder parameter, $g = (1/2)\,(3 - [\langle q^4\rangle]_{\mathrm{av}}/[\langle q^2\rangle]^2_{\mathrm{av}})$, which merge around $\beta = 0.89$. In the low-temperature phase ($\beta > \beta_c$) the curves for different lattice sizes seem to fall on top of each other, but our error bars are still too large to draw a firm conclusion from this quantity.

In Fig. 2 we show that the averaged canonical probability densities $P(q) = [P_i(q)]_{\mathrm{av}}$ reweighted to the transition temperature T_c satisfy the finite-size scaling relation

$$P(q) = L^{\beta/\nu}\hat{P}\big(L^{\beta/\nu}q, L^{1/\nu}(T - T_c)\big)\,, \qquad (5)$$

where $\hat{P}$ is a scaling function, and β and ν are the critical exponents of the order parameter and correlation length, respectively. They are related to $\gamma/\nu = 2 - \eta$ by the standard scaling relation $\beta/\nu = (D - \gamma/\nu)/2$. Using our estimate for γ/ν we thus obtain the value $\beta/\nu = 0.317$ which is employed in Fig. 2. These results are consistent with the findings of Ref. [8] and could be easily improved by redoing the simulations closer to β_c, possibly (using a parallel computer) with more realizations. Narrowing the q range may allow one to simulate lattices of size $L = 16$ and beyond.

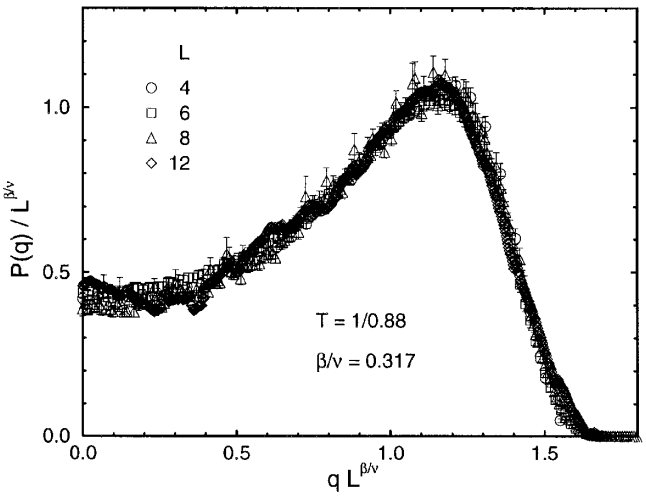

FIG. 2. Scaling plot for $P(q)$ at $1/T = 0.88 \approx 1/T_c$.

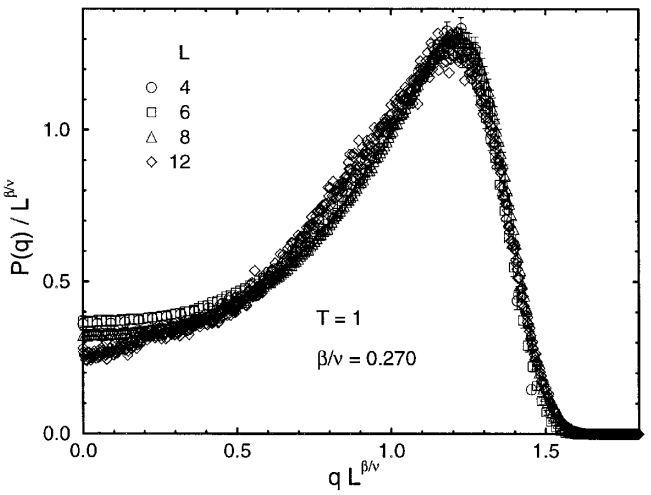

FIG. 3. Scaling plot for $P(q)$ at $1/T = 1$.

The observation that the Binder parameter curves do not splay out at low temperatures suggests that, similar to the 2D XY model, the correlation length ξ may be infinite—or at least larger than the simulated lattice sizes. Generalizing the second argument of $\hat{P}$ to L/ξ and assuming $L/\xi = 0$, we would thus expect that the $P(q)$ should also scale below T_c. By adjusting the only free parameter, $\beta/\nu = 0.270$, we obtained at the simulation point $T = 1$ $(= 0.88T_c)$ the finite-size scaling plot shown in Fig. 3. Moreover, if we reweight our data to the even lower temperatures $T = 1/1.1$ $(= 0.80T_c)$ and $T = 1/1.2$ $(= 0.73T_c)$ we still find a reasonable data collapse if we choose $\beta/\nu = 0.230$ and $\beta/\nu = 0.190$, respectively. Of course, since our lattice sizes are relatively small, we cannot conclude that the correlation length is infinite below T_c. If ξ is large but finite, it is conceivable that we observe an *effective* scaling behavior as long as $\xi > L$. We may conclude that the correlation length is unusually large $(\xi > 12)$ down to $0.73T_c$. However, the slight discrepancy from scaling at $q = 0$ in Fig. 3 ought also to be noted. The value of $P(0) > 0$ turns out to show almost no finite-size dependence, and the qualitative behavior of $P(q)$ is very similar to that in the 4D EAI model [12]. If this behavior would persist asymptotically, it would provide numerical evidence in favor of the Parisi mean-field scenario being valid down to 3D. Note in this context that the results of Ref. [13] are still disputed [14].

Finally, we mention that our method is particularly well suited to study the influence of an interaction term [15] $\epsilon \sum_{i=1}^{N} s_i^1 s_i^2 = \epsilon N q$ in the Hamiltonian (1): We obtain expectation values for arbitrary ϵ values. Physically most interesting is to combine a nonzero magnetic field with a nonzero ϵ value.

In conclusion, we have demonstrated the feasibility of using q-dependent (multioverlap) weight factors. Although the tunneling performance is not optimal, the method opens new horizons for spin glass simulations. In this paper we succeeded, for the first time, to study q barriers in some detail. Using parallel computers and slight modifications of our method (like narrowing the q range, including a magnetic field, etc.) will allow us to extend our investigation into various interesting directions, like an improved study of the thermodynamic limit at and below the freezing point, or ϵ physics.

W. J. acknowledges support from the Deutsche Forschungsgemeinschaft (DFG), and funding through the U.S. Department of Energy enabled his visit to the Florida State University. Major parts of this paper were completed when both authors participated in the research group *Multi-Scale Phenomena* at the ZIF of Bielefeld University. We like to thank the organizers, in particular, Frithjof Karsch, for their hospitality. This research was partially funded by the Department of Energy under Contract No. DE-FG05-87ER40319.

*Electronic address: berg@hep.fsu.edu
†Electronic address: janke@miro.physik.uni-mainz.de

[1] K. Binder and A. P. Young, Rev. Mod. Phys. **58**, 810 (1986); M. Mézard, G. Parisi, and M. A. Virasoro, *Spin Glass Theory and Beyond* (World Scientific, Singapore, 1987); K. H. Fischer and J. A. Hertz, *Spin Glasses* (Cambridge University Press, Cambridge, 1991).
[2] B. A. Berg, in *Multiscale Phenomena and Their Simulation, Proceedings of the International Conference, Bielefeld, 1996*, edited by F. Karsch, B. Monien, and H. Satz (World Scientific, Singapore, 1997), pp. 137–146; W. Janke, in Computer Simulation of Rare Events and the Dynamics of Classical Quantum Condensed Phase Systems, Proceedings of the Summer School and Euroconference, Lerici, Italy, 1997, edited by B. Berne, G. Ciccotti, and D. Coker (to be published).
[3] B. A. Berg and T. Celik, Phys. Rev. Lett. **69**, 2292 (1992); B. A. Berg, U. Hansmann, and T. Celik, Phys. Rev. B **50**, 16 444 (1994).
[4] W. Kerler and P. Rehberg, Phys. Rev. E **50**, 4220 (1994).
[5] K. Hukusima and K. Nemoto, J. Phys. Soc. Jpn. **65**, 1604 (1996).
[6] E. Marinari, G. Parisi, and J. J. Ruiz-Lorenzo, in *Spin Glasses and Random Fields*, edited by A. P. Young (World Scientific, Singapore, 1997).
[7] K. K. Bhattacharya and I. Sethna, cond-mat/9707013.
[8] N. Kawashima and A. P. Young, Phys. Rev. B **53**, R484 (1996).
[9] In this study the realizations are generated according to the condition that J_{ik} takes the values ± 1 with equal probability, which is weaker than $\sum_{\langle ik \rangle} J_{ik} = 0$. The thermodynamic limits are expected to agree.
[10] B. A. Berg, J. Stat. Phys. **82**, 323 (1996).
[11] B. A. Berg, U. Hansmann, and T. Neuhaus, Z. Phys. **90**, 229 (1993).
[12] J. C. Ciria, G. Parisi, and F. Ritort, J. Phys. A **26**, 6731 (1993).
[13] C. Newman and D. Stein, Phys. Rev. Lett. **76**, 515 (1996).
[14] G. Parisi, cond-mat/9603101.
[15] S. Caracciolo, G. Parisi, S. Patarnello, and N. Sourlas, J. Phys. (Paris) **51**, 1877 (1990).